Evolutionary Ecology, 1994, **8**, 74–94

Coevolutionary genetics of hosts and parasites with quantitative inheritance

STEVEN A. FRANK
Department of Ecology and Evolutionary Biology, University of California, Irvine, CA 92717, USA

Summary

A model of host–parasite coevolution is analysed. A host resistance trait and a parasite virulence trait interact to determine the outcome of a parasitic attack, where each trait is determined by quantitative genetic variation. The resistance and virulence traits are assumed to have a fitness cost. Each host and parasite genotype is treated as a separate 'species' in a multidimensional Lotka–Volterra system in which the numerical abundance of each genotype is free to change. Thus, the epidemiological effects of fluctuating population sizes are analysed jointly with changes in genotype frequencies. Population sizes fluctuate increasingly as the parasites' reproductive capacity increases and as resistance and virulence benefits per unit cost decline. The patterns of genetic variability depend mainly on the stability of population sizes and on the shape of the relationship between the costs and benefits of a trait.

Keywords: quantitative genetics; genetic polymorphism; epidemiology; disease; herbivory

Introduction

I analyse a model of host–parasite coevolution. My main goal is to understand the forces that influence quantitative genetic variability in host resistance and parasite virulence. No quantitative genetic model has been published that analyses the genetics of both the host and parasite species.

Quantitative genetic variability for resistance or virulence is often observed in host–parasite systems (Gould, 1983; Mitter and Futuyma, 1983; Burdon, 1987; Christ *et al.*, 1987). Too few studies have been completed, however, to infer any generalities about the genetics of resistance and virulence for quantitative traits. I summarize the relevant empirical literature in the Discussion.

In the model I present here the benefits of resistance in hosts or virulence in parasites may be partly offset by genetically correlated fitness costs. Each host and parasite genotype is treated as an independent 'species' in a multidimensional Lotka–Volterra host–parasite community, which allows free play of both the frequency-dependent forces of host–parasite genetics and the density-dependent forces of epidemiology.

Frequency dependence occurs because the host and parasite traits interact to determine the success of a parasitic attack. For example, a low-cost and low-virulence trait in a parasite may have relatively high fitness when confronted with little resistance among the host population. By contrast, a high-cost and high-virulence trait may be favoured in the parasites when the frequency of resistance increases among hosts.

Density dependence occurs because the net benefit of extra resistance in a host depends on the probability of parasitic attack, that is, on the density of parasites. When parasite density is low, costly resistance traits are of little value, whereas when attack is frequent, it may be that only individuals with costly resistance traits can survive.

These examples of frequency and density dependence suggest that genetic variability cannot be understood outside of an ecological context. Likewise, ecological parameters cannot be

0269–7653

understood outside of a genetical context because population birth and death rates for hosts and parasites depend on the frequency distributions of resistance and virulence traits. The model presented here shows clearly the tightly coupled nature of ecology and genetics in the temporal and spatial patterns of herbivory and disease. (See the Note Added in Proof for additional references.)

Model

The hosts and parasites each have a phenotypic trait that influences the success of a parasitic attack on the host. These traits vary quantitatively and have pleiotropic effects on fitness with the following restrictions: a more resistant host pays a higher fitness cost than a less resistant host; a more effective parasite pays a higher fitness cost than a less effective parasite.

Hosts and parasites each have N different genotypes, with phenotypes that range evenly in value over the interval [0,1] when measured on a particular scale to be defined later. The model is haploid and can be viewed as having either a single locus in a sexual population or many loci in an asexual population.

The dynamics of the system are governed by a discrete-time Lotka–Volterra model (e.g. May, 1974):

$$\begin{aligned} \Delta h_i &= h_i \left(r_i - \sum_i r_i h_i - m \sum_j \lambda_{ij} p_j \right) \\ \Delta p_j &= p_j \left(-s + b_j \sum_i \lambda_{ij} h_i \right) \end{aligned} \tag{1}$$

The genotypes i and j correspond to phenotypic values such that $i, j = 0/(N-1), 1/(N-1), \ldots, (N-1)/(N-1)$. Genotypic indices and phenotypic values are equal. The values of h_i and p_j are the numerical abundances of hosts with genotype i and parasites with genotype j. The model tracks fluctuations in total population sizes (ecological dynamics) and the evolutionary dynamics of genotypic frequencies and phenotypic distributions.

The interpretation of Equation 1 follows the standard Lotka–Volterra convention. The parameter r_i is the ith host genotype's intrinsic rate of increase; $\Sigma_i r_i h_i$ is the effect of competition among hosts for scarce resources, where the carrying capacity is assumed to be 1; m is the morbidity and mortality for a completely successful attack by a parasite; $1 - \lambda_{ij}$ is the amount of resistance to an attack by the jth parasite against the ith host; and b and s are the birth and death rates of the parasite.

Host phenotypes are measured on a scale for the cost of resistance such that $r_i = r(1 - i)$. Parasite phenotypes are measured on a scale for the cost of virulence such that $b_j = b(1 - j)$. These assumptions make the analysis simpler, but the model applies to most situations in which costs of resistance and virulence impose directional selection on phenotypes. For example, let z be the natural metric scale for a host trait and let C specify the mapping between the trait z and fitness cost i, $C(z) = i$, subject to the assumption that C is monotonic in z – that is, selection on cost is directional. Then, after the properties of i are worked out in the model, one can apply $C^{-1}(i) = z$ to establish the properties of the phenotypic distribution on its natural scale.

The most important assumption of the model concerns how host-resistance traits and parasite-virulence traits interact to determine the success of an attack. The assumption is

$$\lambda_{ij} = \begin{cases} \left(\dfrac{j - i - \phi}{1 - \phi} \right)^{\rho} & j - i > \phi \\ 0 & j - i \leq \phi \end{cases} \tag{2}$$

where $-\infty < \phi < 1$ and, hence, $0 \leq \lambda_{ij} \leq 1$. For the jth parasite genotype on the ith host genotype, λ_{ij} is the fraction of the maximal attack rate. The parameter ϕ is the difference between j and i at which the parasite can no longer attack. The value of ϕ affects the slope of the cost–benefit ratio for resistance and virulence traits. The parameter ρ is essentially the rate at which λ_{ij} changes as the difference between host and parasite phenotypes increases, with $\rho > 0$. Figure 1 shows a diagram of λ_{ij}.

The costs and benefits of the disease traits have simple interpretations. For hosts, an increase in i by a small amount ϵ reduces the reproductive rate by the proportion ϵ, but has the benefit of increasing resistance to parasites by the proportion ϵ multiplied by $\partial(1 - \lambda)/\partial i$ evaluated at the point (i,j). Likewise for parasites, an increase in j by a small amount ϵ reduces the birth rate by the proportion ϵ, but has the benefit of increasing the success of attacks by the proportion ϵ multiplied by $\partial\lambda/\partial j$ evaluated at the point (i,j).

Later it will be important to consider whether host resistance increases in an accelerating ($\rho < 1$), linear ($\rho = 1$) or decelerating ($\rho > 1$) manner per unit cost, where these properties are obtained by the sign of $\partial^2(1 - \lambda)/\partial i^2$. Similarly, parasite virulence increases in an accelerating ($\rho > 1$), linear ($\rho = 1$) or decelerating ($\rho < 1$) manner per unit cost, obtained from the sign of $\partial^2\lambda/\partial j^2$.

The model also includes mutation, immigration and extinction. Mutation provides genetic variation in the form of small phenotypic perturbations, immigration provides potentially large genetic and phenotypic perturbations, and extinction deletes from the system unrealistically small abundances of a genotype.

The mutation process follows the step-wise model that has been used successfully in a variety of quantitative genetic analyses (Slatkin, 1987; Frank and Slatkin, 1990). The process can be illustrated by following the changes in the ith host genotype. In each time step, mutation affects abundance, $h'_i = (1 - \mu)h_i + (1/2)\mu(h_{i-\upsilon} + h_{i+\upsilon})$, *where* $\upsilon = 1/(N - 1)$ and μ is the mutation rate. Then disease and selection cause $h''_i = \Delta h'_i + h'_i$ according to the system in Equation 1. The same process is applied to parasites.

Extinction of a genotype occurs when its abundance falls below an arbitrary limit. In the computer analysis reported below, this limit, for both host and parasite, is 10^{-9} multiplied by the carrying capacity of the host.

For immigration, in each time step a uniformly distributed random number between 0 and 1 is chosen. If this number is less than the immigration rate α, then one of the N possible genotypes is chosen randomly and, if its abundance is less than the truncation point for extinctions, then the

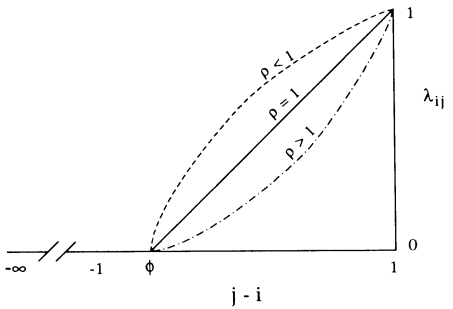

Figure 1. The success of parasite attack as a function of host and parasite genotype. The height, λ_{ij}, is the relative success of an attack, given the difference in genotypic values of parasite and host, $j - i$. The parameter ρ determines the shape of the relationship, ϕ is the value of $j - i$ where $\lambda_{ij} = 0$ and, thus, affects the slope. For $\rho = 1$, $1 - \phi$ is the cost–benefit ratio for alleles affecting resistance or virulence. See Equation 2 for details.

abundance of that genotype is set to a new value: in the computer analysis reported below, the new value is 0.1% of the host's carrying capacity. This process, which is applied independently to the hosts and parasites in each time step, simulates the arrival of occasional immigrants in the local population. Newly introduced genotypes enter into the local population at the same stage in the life cycle as newly recruited progeny born in the local population.

In summary, the model has eight parameters: r, the host's maximum intrinsic rate of increase; m, the maximum morbidity and mortality per infection; b, the parasite's maximum birth rate; s, the parasite's death rate; ϕ, which affects the rate of change in the cost: benefit ratio of resistance or virulence as a function of a metric character, ρ, which determines the shape of the relationship between costs and benefits of disease traits (Fig. 1); μ, the mutation rate; and α, the immigration rate. In addition, the number of genotypes N determines the smoothness of the phenotypic distribution.

Mathematical analysis

The dynamical system in Equation 1 has $2N$ dimensions. The equilibrium for the full system typically has many negative abundances for genotypes, which makes a traditional analysis too complicated to provide any useful clues to the actual behaviour of the system. In this section I outline an approximate mathematical description of the dynamical system. This description provides hypotheses about the dynamics that can be tested by computer simulation.

The main goal is to divide the parameter space into regions, each with particular qualitative properties, and to specify the detailed behaviour of the system whenever possible. The computer simulations serve to test questionable assumptions, to verify the detailed predictions and to fill in the general aspects of the dynamics in regions where a full mathematical analysis is not possible.

The analysis follows these steps.

(1) The hosts are assumed to have a temporally stable distribution of genotypes that is at a fixed point of Equation 1. Given this host distribution, the equilibrium distribution of parasite genotypes is found. It turns out that the parasites will typically be monomorphic for the genotype j^* for any equilibrium distribution of host genotypes.

(2) The assumption is made that, when the system is stable, the hosts are genetically monomorphic for the genotype $i^* = 0$. Given this assumption and the result in step (1), the equilibrium abundance is calculated for the only host genotype present, $\hat{h}_{i^*}$ and for the only parasite genotype present, $\hat{p}_{j^*}$.

(3) The assumption in step (2) is analysed by finding the conditions under which a host genotype $i \neq 0$ can invade when the system is at the point $(\hat{h}_{i^*}, \hat{p}_{j^*})$.

(4) Local stability of the system is analysed from the characteristic equation of the system evaluated at the point $(\hat{h}_{i^*}, \hat{p}_{j^*})$, noting the conditions found in step (3).

(5) The conditions are established under which the hosts are at their carrying capacity, and parasites are absent and unable to invade.

Step 1

The equation for the change in the abundance of the jth parasite genotype is given by Δp_j in Equation 1. The strategy here is to find the value j^* that maximizes Δp_j. If j^* is unique then $\Delta p_k < 0$ for $k \neq j$ because $\Delta p_j = 0$ at equilibrium. Analysing $d(\Delta p_j)/d_j = 0$ yields

$$(1-j)\sum_i \gamma(i)\rho(j-i-\phi)^{\rho-1} - \sum_i \gamma(i)(j-i-\phi)^{\rho} = 0 \qquad (3)$$

where $\gamma(i)$ is the frequency of the ith genotype in the host population and it is assumed that a negligible fraction of the probability mass of i is such that $j^* - i < \phi$. Next, define $\bar{\imath}$ and σ_i^k as the mean and kth central moment of the distribution of i values. Then, by Taylor series expansion,

$$\sum_i \gamma(i)(j-i-\phi)^y = (j-\bar{\imath}-\phi)^y(1+y(y-1)C)$$

$$C = \sum_{k=2}^{\infty} (\sigma_i^k/k!)(j-\bar{\imath}-\phi)^{-k} \prod_{z=2}^{k-1} (y-z)$$

which, upon substitution into Equation 3, yields

$$\frac{(1-j)\rho}{(j-\bar{\imath}-\phi)}\left(1-\frac{2(\rho-1)C}{1+\rho(\rho-1)C}\right)-1 = 0$$

Under the assumption $|2(\rho - 1)C| << 1$, the approximate equilibrium value of j is

$$j^* = \begin{cases} \to 1 & \phi+\bar{\imath}+\rho \geq 1+\rho \\ (\phi+\bar{\imath}+\rho)/(1+\rho) & 0<\phi+\bar{\imath}+\rho<1+\rho \\ 0 & 0 \geq \phi+\bar{\imath}+\rho \end{cases} \quad (4)$$

The approximation is closest when $\rho \to 1$ and, hence, $2(\rho-1)C \to 0$ or when the variation in i is small. Under this condition, j^* is a unique maximum and the phenotypic distribution of the parasites under equilibrium conditions should be very nearly monomorphic at j^*. Stabilizing selection on j occurs because a parasite's growth on a host is the product of its intrinsic birth rate, $b(1-j)$ and its ability to attack that host, λ_{ij}. By contrast, a host's rate of increase, $r(1-i)$ and its resistance, $1 - \lambda_{ij}$, act additively to determine host fitness.

Step 2

It is now assumed that the hosts are genetically monomorphic for $i^* = 0$, which, by the results of the previous section, implies that $j^* = (\phi+\rho)/(1+\rho)$. This reduces the system in Equation 1 to two dimensions, so the equilibrium abundances for hosts and parasites are easily obtained. Defining $K = [(\phi-1)/\phi]^\rho$ and $Z = [(1 + \rho)/\rho]^\rho$, the equilibrium value of h_{i^*} is

$$\hat{h}_{i^*} = \begin{cases} (s/b)Z(1+\rho)/(1-\phi) & -\rho<\phi<1 \\ (s/b)K & \phi \leq -\rho \end{cases} \quad (5)$$

and the equilibrium value of p_{j^*} is

$$\hat{p}_{j^*} = \begin{cases} (r/m)(1-\hat{h}_{i^*})Z & -\rho<\phi<1 \\ (r/m)(1-\hat{h}_{i^*})K & \phi \leq -\rho \end{cases} \quad (6)$$

Step 3

The approximate conditions are developed here under which a monomorphic host population, $i^* = 0$, resists invasion by genotypes $k > 0$ given that the system is temporally stable and at the fixed point $(\hat{h}_{i^*}, \hat{p}_{j^*})$. The approach is to find conditions under which $\Delta h_k < 0$ for all $k > 0$.

The main conclusions are as follows.

(1) For $\rho \geqslant 1$, k cannot invade if $(1 - \hat{h}_{i^*}) < (1 - \phi)\,\rho/(1 + \rho)$ or $-\phi > \rho$.

(2) For $\rho = 1$, the conditions in (1) reduce to k cannot invade if $b(1 - \phi^2) < 8s$ or $-\phi > \rho$. These conditions are sufficient but not necessary for $\rho > 1$; it appears that the system resists invasion by k more strongly as ρ increases.

(3) For $\rho < 1$, a sufficiently small k can invade; details were not obtained on how small k has to be.

(4) For $\rho < 1$, $k = -\phi$ invades if $1 > 1 - \hat{h}_{i^*} > -\phi > \rho > 0$. This requires $(1 + \phi)b(-\phi)^\rho > s(1 - \phi)^\rho$. A stable region where k cannot invade is referred to as a 'cost-free zone' because the least costly host phenotype is favoured; a stable region where some k can invade is referred to as a 'costly zone'.

Some intuition about these conditions can be gained by analysing the marginal changes in costs and benefits of resistance for small changes in i (Simms and Rausher, 1987). When $\rho > 1$, the benefit of resistance increases at a decelerating rate with increasing cost (see above). There are two cases to consider. First, the marginal changes in cost and benefit may be equal at some intermediate optimum, which establishes stabilizing selection on the host resistance traits. Second, the initial increase in benefit for small cost, i near zero, is less than the initial increase in cost. This causes directional selection toward a cost-free phenotype.

When $\rho < 1$, the benefit of resistance increases at an accelerating rate with increasing cost. This may establish disruptive selection on host phenotype, favouring a bimodal distribution of relatively high-cost and low-cost phenotypes in the host population. Alternatively, selection may favour a monomorphic host population with either high-cost or low-cost phenotypes.

Finally, benefits may increase linearly with costs, $\rho = 1$. If initial resistance costs increase more rapidly than benefits when costs are low, then directional selection will favour cost-free host phenotypes. If initial benefits increase more rapidly than costs when costs are low, then the phenotypic distribution may spread across the cost spectrum in an unpredictable way because marginal changes in cost and benefit are equal throughout the phenotypic range. This type of neutral stability in a frequency-dependent model is similar to that found in sex ratio models where there are linear reproductive gains per unit cost (Frank, 1990).

Step 4

The conditions for local stability of $(\hat{h}_{i^*}, \hat{p}_{j^*})$, given that hosts are monomorphic at $i^* = 0$ and parasites are monomorphic at j^* given in Equation 4, are obtained from the largest modulus of the solutions in δ to the characteristic equation

$$\delta^2 + \delta r\hat{h}_{i^*} + mb(1-j^*)\hat{p}_{j^*}\hat{h}_{i^*}\lambda^2_{i^*j^*} = 0 \qquad (7)$$

The parameter space can be divided into stable and unstable zones based on this equation (Fig. 2). The results shown in Fig. 2 were obtained by numerical analysis of Equation 7. For each parameter combination studied, Equation 7 was solved numerically using Mathematica (Wolfram, 1991). The parameter combination was classified as stable if the largest modulus was less than one and unstable otherwise.

Step 5

When parasites are absent, hosts become monomorphic for the genotype $i = 0$, and their abundance approaches the carrying capacity, $h_0 = 1$. A parasite genotype k can invade this monomorphic host population if $\Delta p_k > 0$. The conditions for k to invade are straightforward and require no special assumptions

$$1-\phi > \frac{s(1+\rho)}{b}\left(\frac{1+\rho}{\rho}\right)^{\rho} \qquad 1-\phi<1+\rho$$
$$\left(\frac{-\phi}{1-\phi}\right)^{\rho} > \frac{s}{b} \qquad 1-\phi \geq 1+\rho \tag{8}$$

where $k = (\phi + \rho)/(1 + \rho)$ if $1 - \phi < 1 + \rho$ and $k = 0$ if $1 - \phi \geq 1 + \rho$. These conditions are equivalent to $\hat{h}_{i^*} < 1$ (see Equation 5). The condition for invasion of parasites determines the lower surface in Fig. 2.

Computer analysis

Methods and summary statistics

Design and analysis of simulations Each *run* of the computer model has particular values assigned to all of the parameters described above. The model begins with a single empty patch containing no hosts or parasites. The patch is colonized during the following 2000 generations by the immigration process described above.

Each *generation* is one turn through the life cycle, which includes one application of Equation 1 to the abundances of hosts and parasites. Because Equation 1 can be interpreted in a variety of ways, the mean life span of an individual can be longer than one turn through the life cycle but, in this paper, I ignore issues that concern overlapping generations and age structure.

No statistics are collected during the initial 2000 generations of each run. In each of the following 5000 generations, statistics are collected on the abundance of hosts and parasites, the variability in phenotypic values and other measures described later. The run is completed at the end of these 5000 generations and, for each statistic, there are 5000 values that form a temporal distribution for that run. Each distribution is summarized by its 5th, 25th, 50th, 75th and 95th percentiles – I sometimes refer to the 50th percentile as the median.

Each *design* is a set of runs with parameters defined by a factorial combination of values. For example, if the parameters s, ϕ, b and r were each varied over three levels, then the design would have 3^4 runs. The output for this design would consist of 3^4 values for each of the five percentile

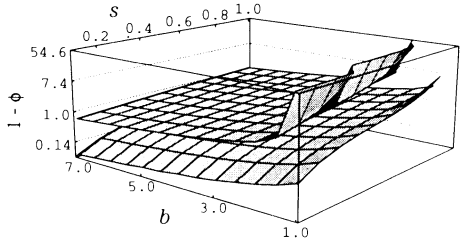

Figure 2. Predicted spaces of stability and instability for the dynamical system in Equation 1 based on the characteristic equation in Equation 7. Parameter combinations between the surfaces yield stable host and parasite abundances, combinations above the upper surface yield fluctuating abundances and combinations below the lower surface yield absence of parasites. The conditions for stability are independent of m and depend weakly on r. Values shown are for $r = 1$; for $r = 16$ the upper surface rises slightly, but the difference is barely perceptible between $r = 1$, shown here, and $r = 16$. The conditions for stability also depend weakly on ρ over the range [0.5, 2.0]: higher values of ρ raise both surfaces by an amount that is barely perceptible over this range. Values for $\rho = 1$ are shown. The grid shows values of s that vary over the range [0.1, 1.0] by steps of 0.1 and values of b that vary over the range [1.0, 7.0] by steps of 0.5.

levels for each of the statistics collected. Parameter values for particular designs are given in the legends of figures where the results are presented. For all designs the number of genotypes, N, is set to 255, which provides a reasonable approximation to a continuous distribution of phenotypes.

Some useful measures for genetic variability The cost of resistance for a particular host individual is the value of its genotype, i. Thus variability in fitness caused by the cost of resistance is approximately the amount of variability in $(1 - i)/(1 - \bar{\imath})$. Similarly, the cost of virulence for a pathogen is j, and variability in fitness due to cost is approximately the variability in $(1 - j)/(1 - \bar{\jmath})$. These measures will be referred to as variability in standardized costs.

The next step is to measure genetic variability in the benefits of resistance and virulence. The amount of susceptibility of host genotype i relative to the mean in the population is $E_j(\lambda_{ij})/E_{ij}(\lambda_{ij})$, where E_j is the expectation over j and E_{ij} is the expectation over i and j. A similar measure is constructed for parasites. The amount of virulence to a mean host for the jth parasite genotype is $E_i(\lambda_{ij})$, and the measure of the virulence of j relative to the mean given the present host and parasite distributions is $E_i(\lambda_{ij})/E_{ij}(\lambda_{ij})$. Variability in this measure will be referred to as variability in standardized benefits.

Characteristics of the system under ecological stability

Population abundances According to the analytic theory, the stability of population abundances depends mainly on three parameters: parasite recruitment and death rates, b and s and the slope of the cost–benefit ratio for resistance and virulence traits over the range of phenotypes, which depends on $1 - \phi$. Three regions of the parameter space are shown in Fig. 2. Below the lower surface parasites are typically absent and hosts are at their carrying capacity. Between the surfaces population abundances are typically stable with both hosts and parasites present. Above the upper surface population abundances of hosts and parasites typically fluctuate over time.

The simulation model confirms the analytical theory's division of the parameter space into three regions with differing stability properties (Fig. 3). The theory given in step 3 of the Mathematical analysis subdivides the stable region between the surfaces into two zones. In the cost-free zone the hosts are predicted to be monomorphic for the minimum cost phenotype, $i^* = 0$, and the predicted abundances for hosts and parasites are given in Equations 5 and 6. In the costly zone the distribution of host genotypes cannot be predicted exactly and no clear predictions for population abundances were derived. The transition between the cost-free and costly zones is expected to occur such that, when $\rho = 1$, cost-free monomorphism holds when $b\,(1 - \phi^2) \leqslant 8s$.

For each run with parameters between the surfaces in Fig. 3, I calculated the observed median abundances minus the predicted values and divided this difference by the predicted value (standardized difference). For 425 parameter combinations in the cost-free zone, where the predictions are expected to hold, the means and standard deviations of the standardized differences were 0.01 ± 0.02 for hosts and -0.03 ± 0.04 for parasites. (These combinations exclude points at which $b = 1$ and $s = 0.8$ (see caption of Fig. 3). For 93 parameter combinations in the costly zone, where the predictions are not expected to hold, the means and standard deviations of the standardized differences were 0.85 ± 0.79 for hosts and -0.32 ± 0.17 for parasites.

Genotypic distributions The previous section described two regions of the parameter space between the surfaces shown in Fig. 3. The analytic theory predicts that, in the cost free zone, very little genetic variability will be maintained for the fitness costs and benefits of resistance and

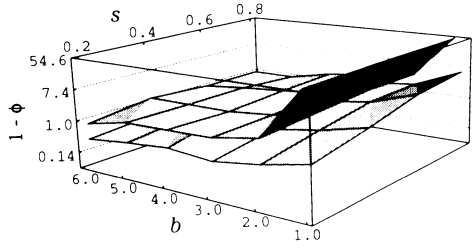

Figure 3. Observed spaces of stability and instability from the computer-simulation model. The interpretation of the figure is the same as Fig. 2, with the following changes. The parameters of the simulation were: $m = 0.2$, $\rho = 1$, $r = 2$, $\mu = 10^{-4}$ and $\alpha = 0.01$. A slightly smaller range of values for s and b is shown here compared with Fig. 2: here the grid shows values of s that vary over the range [0.2, 0.8] by steps of 0.2 and values of b that vary over the range [1.0, 6.0] by steps of 1.0. Zones of stability, instability and parasite extinction were determined by varying $1 - \phi$ over the range [0.1, 10.9] by steps of 0.1 for each (b, s) pair. A point was considered stable if, in a simulation run, for both hosts and parasites (1) the median abundances were greater than 0.01, (2) the differences between the 75th and 25th percentiles in abundance were less than d, where d is the greater of 0.1 and 0.1 multiplied by the median abundance and (3) the differences between the 95th and 5th percentiles in abundance were less than e, where e is the greater of 0.2 and 0.2 multiplied by the median abundance. The surfaces are the highest and lowest values of $1 - \phi$ that are stable. Non-stable points by these criteria occur between the surfaces. For the 521 internal points tested, 114 were not stable, but 40 of these occurred when $b = 1$ and $s = 0.8$. Smaller values of e and d (for example, $d = 0.02$ and $e = 0.05$) cause only a barely noticeable difference in the location of the surfaces, but have more internal exceptions.

virulence traits. The mean cost for hosts is predicted to be near zero and for parasites to follow Equation 4. In the costly zone, the parasites are still predicted to have low variability and to follow Equation 4, approximately, but the mean and variability in host resistance traits could not be predicted for $\rho = 1$.

I compiled information for each run of the parameter combinations between the surfaces of Fig. 3. I summarized three statistics: the mean cost, measured by the mean value of i for hosts and the mean value of j for parasites, the standard deviations in the standardized costs and the standard deviations in the standardized benefits (see above). Recall that each statistic is calculated in each generation of a run and then the 5th, 25th, 50th, 75th and 95th percentiles of these statistics are calculated over generations for each run. To summarize the information, the percentiles over runs for these statistics can be examined, for example, the median or 95th percentile over runs for the 5th, 50th and 95th percentiles within each run.

In the cost-free zone, the hosts' mean cost of resistance is near zero and there is little variation in the population. The medians over runs of the 50th and 95th percentiles for the mean cost of resistance in hosts are 0 and 0.02, respectively; the 95th percentiles over runs of the 50th and 95th percentiles are 0.03 and 0.12, respectively. Thus the cost is typically close to 0 as predicted. The standard deviations of standardized costs and benefits for hosts are also very close to 0 as shown by an upper bound: the 95th percentile over runs for the 95th percentile within runs is 0.01 for both measures.

The mean and variance in fitness costs for hosts in the costly zone can be summarized by 5th, 25th, 50th, 75th and 95th percentiles over runs for the 50th percentile in the mean costs and the standard deviation of standardized costs and benefits within each run. For the mean costs these percentiles are 0.02, 0.09, 0.19, 0.29 and 0.44, for the standard deviations of the standardized

costs these percentiles are 0.01, 0.04, 0.11, 0.20 and 0.28; and for the standard deviations of the standardized benefits these percentiles are 0.02, 0.17, 0.26, 0.33 and 0.52. There is a trend of increasing mean and standard deviation in costs and benefits with increasing distance from the transition between the cost-free and costly zones (Fig. 4).

The mean cost for parasites follows the predictions in Equation 4 fairly closely. To measure the fit I subtracted the predicted value from the observed median for each run, then calculated the mean plus or minus the standard deviation of this difference over all combinations in the cost-free and costly zones, which is 0.02 ± 0.03.

The variance in fitness costs and benefits for parasites is low in the cost-free zone. The 50th and 95th percentiles over runs of the 95th percentile in each run for the standard deviation of the standardized costs are 0.01 and 0.05, respectively, with values 10–20% smaller for standard deviations in standardized benefits.

The genetic variability of the parasites is typically low even in the costly zone, although in a few cases there is moderate variability. For standard deviations in standardized costs, the 50th and 95th percentiles over runs for the 50th percentile in each run are 0.02 and 0.13, respectively, and for the 95th percentile in each run are 0.06 and 0.27, respectively. Values are 10–20% smaller for standard deviations in standardized benefits.

The distribution of host genotypes in the costly zone remains almost constant over generations within a run. However, the host genotypes stabilize at different distributions among runs that have the same parameters but different seeds for the random number generator (see step 3 of Mathematical analysis). To illustrate this I chose four parameter combinations in the costly zone, ran three replicates of each combination and plotted the results in Fig. 4. This figure also shows that the distribution of host genotypes often has a strongly bimodal shape and that the mean cost

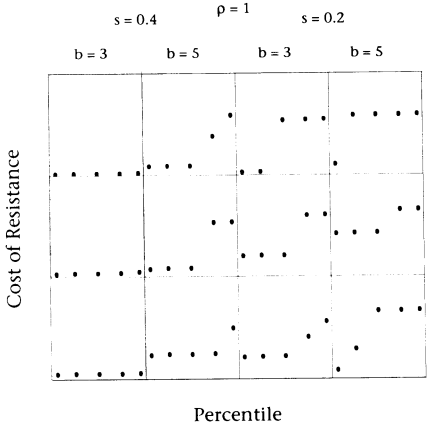

Figure 4. The distribution of host genotypes in the costly, stable zone of the parameter space with a linear cost–benefit relationship. The rows of plots are replicates for particular parameter combinations in each column. The parameters are the same as listed in Fig. 3, with $1 - \phi = 0$. The distance from the transition between cost-free and costly zones increases from left to right. The y axis of each plot shows the cost of resistance associated with a genotype, ranging from 0 to 0.8. The x axis has the following interpretation: In each generation of a run, the 5th, 25th, 50th, 75th and 95th percentiles are calculated for the distribution of the cost of resistance within the host population. Each percentile class is recorded for each of 5000 consecutive generations in a run. The median over time for each class is plotted; the left point in each panel is the median of the 5th percentile and the right point is the median of the 95th percentile. The distributions are stable over time within a run.

of resistance increases with increasing distance from the transition between the cost-free and costly zones. The variability in outcome among different replicates with the same parameters is probably caused by neutral stability under a linear cost–benefit relationship, $\rho = 1$ (see step 3 of Mathematical analysis).

Shape of the cost–benefit relationship The Mathematical analysis suggested that the shape of the cost–benefit relationship, determined by ρ, would influence the mean and the variation in resistance costs and benefits for the hosts. In particular, decelerating resistance benefits per unit cost, $\rho > 1$, are expected to cause either directional selection toward a cost-free phenotype if the parameters are in the cost-free zone or stabilizing selection toward an intermediate optimum in the costly zone. Accelerating resistance benefits per unit cost, $\rho < 1$, are expected to cause disruptive selection on the hosts. Finally, linear benefits per unit cost, $\rho = 1$, are expected to cause directional selection for cost-free phenotypes for parameters in the cost-free zone or a variety of host distributions reflecting neutral stability for parameters in the costly zone.

The results in the previous section support the predictions of the Mathematical analysis for $\rho = 1$. In this section the predictions for non-linear returns are compared with simulation results. The simulation design is the same as in Fig. 3 except that ρ is either 0.5 or 2.0.

The surfaces defining the stable zone have the same shape as in Fig. 3 for $\rho = 0.5$, 2. Both surfaces raise slightly on the scale in Fig. 3 as ρ increases over the values 0.5, 1 and 2, as predicted by the analytic theory in steps 4 and 5 of the Mathematical analysis.

Within the stable zone the equilibrium abundances and genotypic distributions depend on whether a parameter combination falls into the cost-free or costly region as discussed above. In this design the transition between cost-free and costly zones that gives a good fit to the simulations is slightly different from that predicted by Step 3 of the Mathematical analysis. For $\rho = 0.5$, the transition is described well by the condition for cost-free monomorphism of $1 - \hat{h}_{i^*} < (1 - \phi)\rho/(1 + \rho)$, where $\hat{h}_{i^*}$ is given in Equation 5. For $\rho = 2$, the transition is described well by the condition for cost-free monomorphism of $b\,(1 - \phi^2) < 8s$. The main conclusions for $\rho = 1$ hold for the larger and smaller values of ρ in this design. The only significant changes in results with changing values of ρ occur for the distribution of host genotypes in the costly zone and the distribution of parasite genotypes when the hosts respond to disruptive selection.

The simulations show the expected trend toward reduction in the host population's genetic variance for the transition from disruptive to neutral to stabilizing selection on host phenotype when the parameter combination is in the costly zone. This can be illustrated by examining the 50th percentile within runs for the standard deviations in standardized costs. For ρ values of 0.5, 1 and 2, the medians over parameter combinations were 0.19, 0.10 and 0.01, respectively. The small variance for $\rho = 2$ is consistent with the prediction of stabilizing selection for $\rho > 1$. The neutral stability of the genotypic distribution and the intermediate variance for $\rho = 1$ also follow the predicted trend (Fig. 4). Finally, the results for $\rho = 0.5$ show the expected pattern for the host distribution of larger variance, bimodal shape and strong stability compared with $\rho = 1$ (compare Figs 4 and 5).

The mean cost for hosts can be high and the genetic variance low when there is stabilizing selection toward an intermediate optimum. For example, the 50th and 95th percentiles over runs of the median cost within runs are 0.15 and 0.41, respectively, for parameter combinations in the costly zone and $\rho = 2$.

The genetic variability in parasites is low except when there is disruptive selection on hosts, $\rho < 1$ (Fig. 5). This can be illustrated by examining the 50th percentile within runs for the standard deviations in standardized costs for the parasite population. For ρ values of 0.5, 1 and 2, the medians over parameter combinations were 0.15, 0.02 and 0.01, respectively.

Role of other parameters in the stable zone. The effects of varying r and m were studied next. The simulation design was the same as in Fig. 3 except that m was either 0.1 or 0.4 and r was varied between 1 and 4 in a pattern orthogonal to m.

The surfaces defining the stable zone have the same shape as in Fig. 3. The parameter m has no detectable effect on the location of the surfaces, low r ($r = 1$) has approximately the same surfaces of stability as shown in Fig. 3, and high r ($r = 4$) has a similar upper surface but has a significantly raised lower surface, reducing the zone of stability in the volume between the surfaces.

Within the stable zone the equilibrium abundances and genotypic distributions depend on whether a parameter combination falls into the cost-free or costly region as discussed above. The computer simulations with varying r and m support the transition between the cost-free and costly zones and the qualitative patterns of abundance and polymorphism predicted by the Mathematical analysis. For parameter combinations in the costly zone, the mean resistance cost and the amount of genetic variability for the hosts increase with higher r values (medians over runs approximately 25–100 % greater), and are not affected by m. Parasite variability is not significantly affected by either r or m.

Dynamics under ecological instability

The abundances of hosts and parasites fluctuate over time when the parameters are above the upper surface of Fig. 2. A qualitative analysis can be made by examining the system's behaviour as parameter combinations move steadily upward from the upper surface. Two parameter sets were chosen based on Fig. 3, on a search through the parameter space in the unstable zone and on the analysis outlined above. In each set the dynamics are summarized for parameters that start just above the surface of Fig. 3 and then move steadily upwards by increasing $1 - \phi$ and holding the other parameters constant.

Linear cost–benefit relationship. In the first case there is a linear relationship between fitness costs and benefits, $\rho = 1$. Figure 6 shows the dynamics when the system is just above the surface in Fig. 3 and is in the transition between ecological stability and instability. The time series and phase plane for host and parasite abundances show that the system has nearly steady population sizes

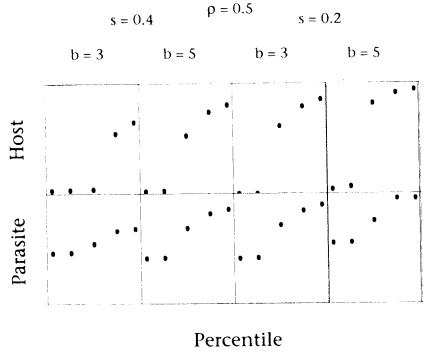

Figure 5. The distribution of host and parasite genotypes in the costly, stable zone of the parameter space with disruptive selection ($\rho < 1$) on the hosts. This plot is similar to Fig. 4 except that $\rho = 0.5$, the top row is for the cost of resistance in the host and the bottom row is for the cost of virulence or aggressiveness in the parasite. The patterns are consistent across replicates for the same parameters, so only one replicate for each combination is shown.

for over 2000 generations and then spirals out to three successive patterns of almost steady cyclical behaviour. This is the typical bifurcation that characterizes the transition from a locally stable equilibrium point to locally unstable equilibrium in non-linear systems (Guckenheimer and Holmes, 1983). For these parameters the mean genotypic values are almost steady over time in spite of constant mutations of small effect and the occasional introduction of widely varying genotypes. There is almost no genetic variability (standard deviation near 0).

As the parameters move steadily upwards from the surface of Fig. 3, the dynamics of the population abundances are characterized by stable limit cycles that increase in radius as $1 - \phi$ increases. The mean genotypic values are steady over time and the standard deviations are near 0.

As the orbits increase in radius the trajectories approach the boundary where the abundance of hosts is near 0 on each turn through the phase plane (the direction of the orbits is counter-clockwise). In the simulations the hosts are assumed to be extinct when their abundance falls below an arbitrary truncation point. For these runs the truncation point was 10^{-9} multiplied by the host's carrying capacity in the absence of parasites. Figure 7 shows the dynamics where the

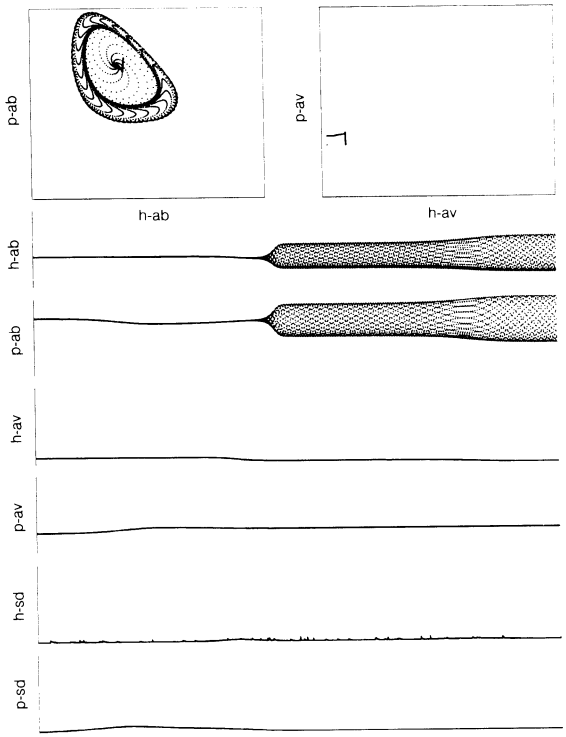

Figure 6. Temporal dynamics near the transition between ecological stability and instability. The upper left panel is the phase plane for host (h-ab) and parasite (p-ab) population abundances. The upper right panel is the phase plane for host (h-av) and parasite (p-av) mean genotypic values. The six plots below are time series over the 5000 generations of the simulation run for the four measures given above plus the standardized standard deviations in fitness costs for hosts (h-sd) and parasites (p-sd). The standard deviations provide a measure of genetic variability. The scale in each plot is between zero and one, except for p-ab which ranges between zero and the maximum value observed over the 5000 generations, p-max, which was 17.9 for this run. The parameters common to this and figs 7–10 are $m = 0.2$, $r = 2$, $b = 5$, $s = 0.6$, $\alpha = 0.01$ and $\mu = 10^{-4}$. For this run $\rho = 1$ and $1 - \phi = 1.4$.

trajectories are almost stable limit cycles for hundreds of generations but then the hosts become extinct and the system may oscillate through short periods of extinction followed by recolonizations and then extinction once again.

The mean genotypic values vary widely over time in this region of the parameter space. Each new colonization of hosts begins with a genotypic value taken from a uniform distribution over [0,1]. The mean genotypic value then evolves by small mutations and by the arrival of immigrants with widely varying genotypes. A similar process applies to the colonization and evolution of parasite genotypes.

The widely varying genotypic values over time within a patch may allow a metapopulation to maintain a great deal of genetic variability even though each patch typically has low genetic diversity. Under more realistic migration and macromutation schemes, however, the amount of genetic variability over time and space may be lower than shown here.

Finally, as the parameter combination moves farther above the surface of Fig. 3, the dynamics are characterized by repeated colonization–extinction cycles (Fig. 8). The dynamics are controlled mainly by the timing and the genotypic distribution of the colonists.

Non-linear cost–benefit relationship. When $\rho = 2$ (see Fig. 1) the dynamics follow the qualitative patterns described above for a linear cost–benefit relationship. When $\rho = 0.5$, considerably more genetic variability is maintained when the parameters are near the transition between ecological stability and instability. Figure 9 shows the dynamics with $1 - \phi$ just above the stability–instability transition. The time series for abundances show the system moving between periods of

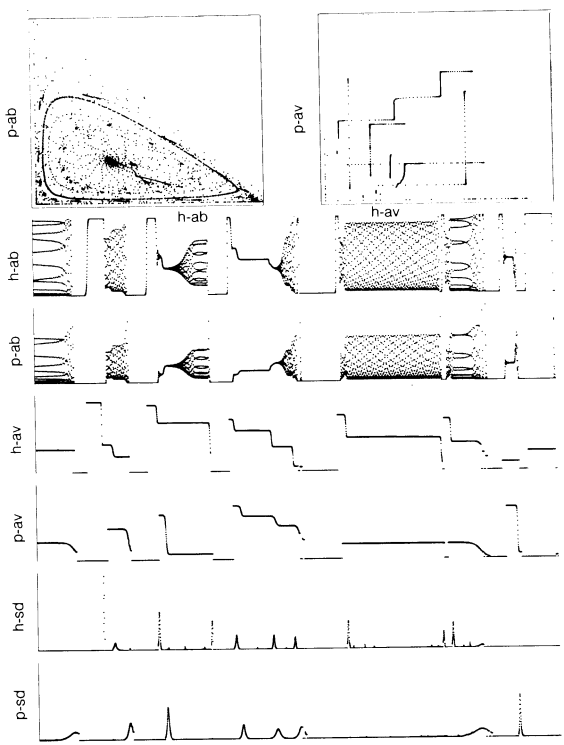

Figure 7. Temporal dynamics for $\rho = 1$, $1 - \phi = 2.5$ and p-max = 28.8. Other aspects of the figure are explained in the legend of Fig. 6.

cycling and almost steady behaviour in population sizes. The hosts' mean genotypic value fluctuates rapidly over a small range when the populations sizes are cycling. Perhaps the most interesting result is that the hosts maintain a significant amount of genetic variability, which is consistent with the results for $\rho = 0.5$ in certain parts of the stable zone (see above).

With a small increase in $1 - \phi$ into the unstable zone the hosts no longer maintain much genetic polymorphism within a patch (Fig. 10). As $1 - \phi$ continues to increase the stable cycles break up into more frequent colonization–extinction oscillations similar to Fig. 8, where the mean genotypic values vary over time.

General comments about dynamics in the unstable zone. I list a few general observations in this section.

(1) When a patch is empty any host genotype (any i) can invade and increase to the carrying capacity fairly quickly.

(2) When the host is at its carrying capacity a parasite can invade if $-s + b\,(1 - j)\lambda_{ij} > 0$, which implies that $b\,(1 - j) > s$ is a necessary but not sufficient condition. This condition is easier to satisfy as λ_{ij} increases and, hence, as $1 - \phi$ increases and ρ decreases.

(3) Stable cycles are more likely as the equilibrium point for host abundance, $\hat{h}_{i^*}$, increases, since low values of $\hat{h}_{i^*}$, are more likely to move the orbits of a cycle closer to the $h = 0$ boundary.

(4) Almost stable cycles formed after each new colonization event will often have a different orbit. This occurs because each new colonization changes the dominant host or parasite

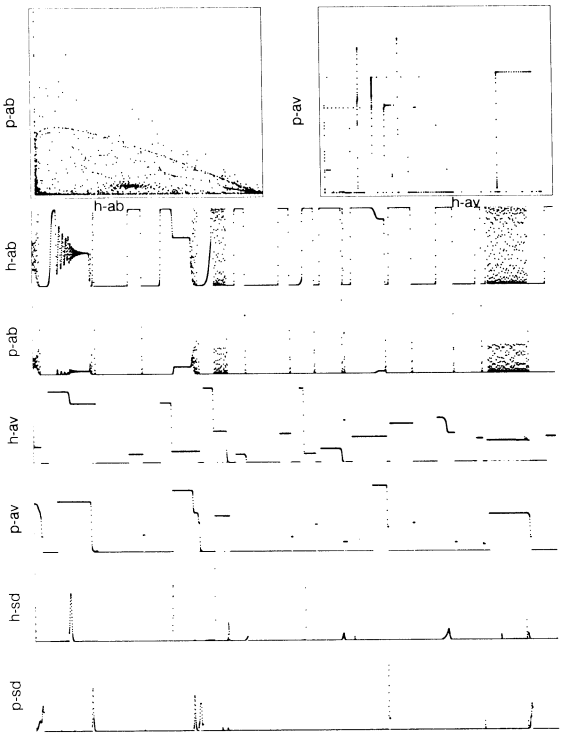

Figure 8. Temporal dynamics for $\rho = 1$, $1 - \phi = 6$ and p-max = 35.1. Other aspects of the figure are explained in the legend of Fig. 6.

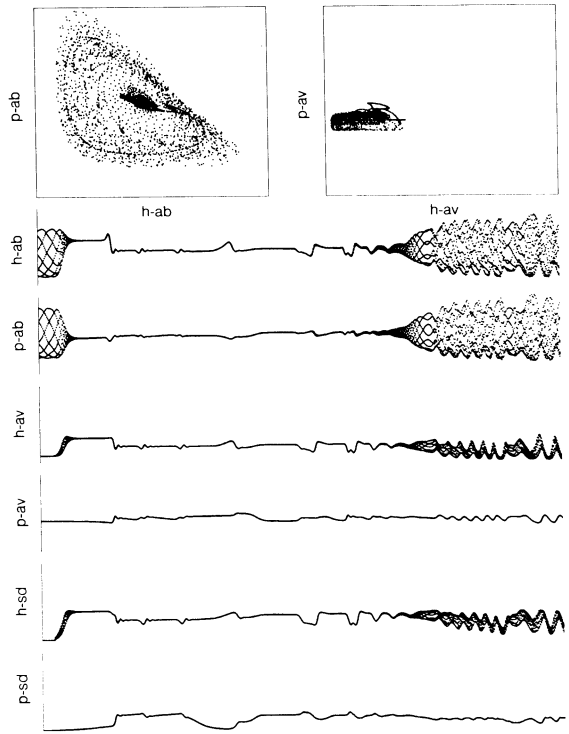

Figure 9. Temporal dynamics for $\rho = 0.5$, $1 - \phi = 1.1$ and p-max = 18.1. Other aspects of the figure are explained in the legend of Fig. 6.

genotype, which in turn changes a key parameter of what is essentially a two-dimensional host–parasite system. Changes in key parameters can also occur by a slow response to selection acting on the quantitative genetic variability caused by mutations of small effect, as appears to happen in Figs 6 and 10.

Discussion

Summary of main results

Ecological stability. The stability of population sizes in this model depends on the parasites' birth and death rates (b and s). Parasites with explosive growth are more likely to cause population cycles or extinction of the hosts. Stability also depends on the slope of the benefit–cost ratio for the host resistance trait or the parasite virulence trait. The benefit–cost ratio is inversely related to the parameter $1 - \phi$ (Equation 2, Fig. 1).

The effects of the parasite vital rates and the benefit–cost ratio are shown in Figs 2 and 3. Below the lower surface parasites are absent from the system. Between the surfaces the sizes of the host and parasite populations are stable over time. As the parameters move just above the upper surface, with $1 - \phi$ increasing, the population sizes cycle over time (Figs 6 and 9). These cycles expand in amplitude as $1 - \phi$ continues to increase until limit cycles are replaced by repeated host extinctions, caused by explosive growth of the parasites and subsequent recolonization of the empty patch by immigrant hosts (Fig. 8).

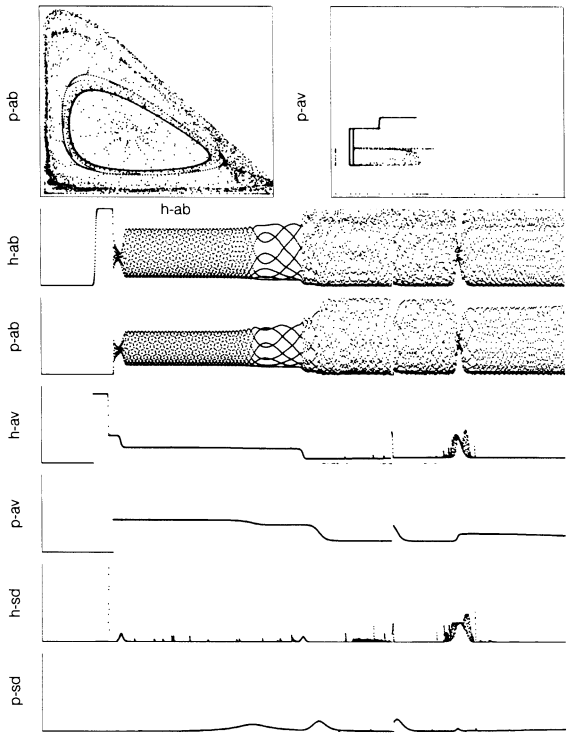

Figure 10. Temporal dynamics for $\rho = 0.5$, $1 - \phi = 1.3$ and p-max = 24.2. Other aspects of the figure are explained in the legend of Fig. 6.

Genetic variability under ecological stability Genetic variability of the hosts under ecological stability depends primarily on the interaction between two factors. First, whether any variability occurs is typically determined by whether a costly resistance trait can invade a host population that is fixed for the cost-free phenotype. Detailed conditions were provided for when such invasion occurs (see Mathematical analysis); the intuitive meaning of these details is simply that the initial benefit of increased resistance depends on the abundance of parasites, the distribution of parasite genotypes and the rate at which resistance benefits increase per unit cost. Parameter combinations can be classified according to whether they cause stability of cost-free host phenotypes or allow invasion of costly resistance.

The second, related factor that determines genetic variability of the host is the shape of the cost–benefit relationship for resistance traits. If benefits increase at a decelerating rate and an initial costly resistance trait can invade, then stabilizing selection on the host population favours an intermediate-cost phenotype with little genetic variability. If benefits increase at an accelerating rate and an initial costly resistance trait can invade, then disruptive selection on the host population causes a bimodal distribution of host phenotypes and the maintenance of considerable genetic variability (Fig. 5). With accelerating benefits the quantitative trait acts approximately as a threshold character with essentially qualitative effects on resistance. The polymorphism observed in this case is analogous to the polymorphism in qualitative models of resistance (Leonard and Czochor, 1980; Frank, 1992, 1993).

Genetic variability in the parasites depends on the interaction between two factors. First, there

is an inherent tendency toward stabilizing selection on parasite virulence or aggressiveness characters. This occurs because a parasite's reproductive rate is the product of its intrinsic reproductive capacity, which is reduced by the cost of virulence, and its ability to attack hosts, which increases with the costliness of its virulence trait. Roughly speaking, if x is the cost of virulence which ranges between 0 and 1, then intrinsic reproductive capacity changes according to $(1 - x)$ and attack success changes according to x, so overall reproduction depends on $x(1 - x)$, which is a stabilizing selection function. An accelerating gain in virulence per unit cost would establish an opposing disruptive tendency but, in general, the net effect tends toward an overall stabilizing selection function that favours an intermediate optimum with little genetic variation.

The second factor that affects parasite variability is the distribution of host genotypes. When the hosts experience disruptive selection and have a bimodal phenotypic distribution, the parasites in turn show a tendency toward bimodality (Fig. 5).

Genetic variability under ecological instability. The main conclusions from the analysis are as follows.

(1) Parasite phenotypes typically evolve to an intermediate optimum when local extinctions are rare (Equation 4, Figs 6 and 9). When the system is ecologically unstable and the mean resistance value of the hosts fluctuates (see below), the parasite optimum may fluctuate rapidly with small amplitude (Fig. 9) or slowly over a wide range (Fig. 10).

(2) Host resistance typically evolves to a level of minimum cost and minimum benefit whenever local extinctions are rare and resistance benefits increase in a linear or decelerating (stabilizing) way per unit cost (Fig. 6, step 3 of Mathematical analysis). Either intermediate cost and low variability or a bimodal distribution of host phenotypes can evolve for some parameter combinations, depending on the slope of the cost–benefit relationship.

(3) Intermediate levels of host cost and benefit and considerable genetic variability for resistance evolve when selection on host phenotypes is disruptive and local extinctions of populations are rare (Fig. 9). Some genetic variability among parasites is often maintained under these conditions (Fig. 9).

(4) Frequent extinction–recolonization cycles can lead to large differences in genetic composition over time but limited variability at any particular time (Figs 7 and 8). This occurs because each new colonization cycle may start with any genotype over a wide range of phenotypic values. Following each colonization, mean phenotypic values continue to change over time until the next extinction. In a region where many local populations have colonization–extinction dynamics, the genetic variability over space can be quite high (Frank, 1991a). In this case the outcome depends on the details of the mutation and migration processes.

Relation to past theory

No previous work has analysed the coevolutionary responses of both hosts and parasites with continuously varying traits (see reviews by Gould, 1983; Mitter and Futuyma, 1983; Simms and Fritz, 1990). The main line of thinking in past theory has been to assume a fixed parasite population and then to consider possible evolutionary responses by the hosts. For example, several authors have considered a verbal model that assumes the benefits of resistance increase at a decelerating rate with increasing costs. They concluded that stabilizing selection on the host resistance trait would lead to an intermediate optimum with the potential for genetic variability. This theory was summarized by Simms and Rausher (1987). Simms and Fritz (1990) noted, however, that stabilizing selection of this type would probably not maintain much genetic variability, a conclusion supported by the results derived here.

The model presented here is an extension of the typical Lotka–Volterra equations for an interaction between one host species and one parasite species (e.g. May, 1974). Specifically,

instead of a pair of interacting species, there are N host genotypes and N parasite genotypes. The dynamics of Lotka–Volterra models with high dimensionality have been examined in only a few cases (Hamilton, 1986; Frank, 1991a,b, 1993) and in those cases the different host and parasite genotypes had qualitatively different traits rather than the almost continuous variation analysed here. The models with qualitatively different phenotypes often support more genetic variation than in the quantitative model because of the inherently disruptive (discontinuous) nature of qualitative resistance and virulence.

The present model can also be related to known theory by noting that, as the increase in benefits per unit cost approaches 0, the $2N$ dimensional system reduces to the standard two-dimensional host–parasite system. This can be seen by examining Equations 1 and 2: host and parasite success are independent of genotype when $1 - \phi$ approaches infinity. The value of $1 - \phi$ is approximately inversely proportional to benefits of resistance or virulence traits per unit cost. The stabilizing effects of quantitative genetic variability on ecological dynamics can be seen in Fig. 2 by the increase in the area of stability as $1 - \phi$ decreases from infinity to intermediate values at which resistance and virulence traits can be effective.

Observations and future directions

The model presented here is the first step toward a realistic theory. The fact that the model sometimes supported little genetic variability whereas natural systems appear to maintain variability (Gould, 1983; Berenbaum and Zangerl, 1992; Kennedy and Barbour, 1992) suggests that theoretical extensions and empirical detail are needed. Comparisons with the few available data suggest how the theory may be extended.

Costs of resistance and virulence are assumed to be a central component of host–parasite coevolution in theories with quantitative genetics (Simms and Fritz, 1990) and qualitative genetics (Leonard and Czochor, 1980; Frank, 1992). The reason for this assumption is clear: without an opposing selection pressure, all genetic variation for resistance and virulence would be depleted apart from the transient fixations of new, advantageous alleles (Leonard and Czochor, 1980; Rausher and Simms, 1989). Costs are observed in some empirical studies but not in others (Leonard and Czochor, 1980; Simms and Rausher, 1989; Simms and Fritz, 1990; Frank 1992; Marquis and Alexander, 1992).

It is useful to distinguish three types of cost. *Structural and metabolic costs* are the energy required to make and maintain defensive structures or chemicals. Berenbaum *et al.* (1986) showed that resistance of wild parsnips to the parsnip webworm depends on an array of defensive chemicals. In the absence of herbivory, those plants with relatively high resistance had relatively low fecundity. Variation in the levels of defensive compounds was highly heritable and polygenic.

Strong reciprocal evolution of plant and herbivore is likely in Berenbaum *et al.*'s (1986) system because wild parsnip is the primary host for the parsnip webworm and the parsnip webworm is the primary herbivore of wild parsnip. The costs of resistance, the quantitative inheritance and the two-species interaction match the assumptions of the model presented here. However, one class of defensive chemical (furanocoumarins) was advantageous when in seeds but disadvantageous when in leaves. Berenbaum *et al.* (1986) suggest that furanocoumarins have a defensive effect in seeds but act as an attractant for herbivores when in the leaves. This work suggests that the trade-off between defence and attractiveness is an interesting direction for future empirical and theoretical work.

Life history costs arise when fecundity, timing of reproduction or other fitness components are correlated with success in the host–parasite battle. For example, the dioecious, perennial herb *Silene alba* is attacked by the anther-smut fungus *Ustilago violacea*, which causes both male and female plants to produce anthers that carry fungal spores instead of pollen (Alexander, 1990). The spores are transmitted mainly by insect pollinators; the system thus has the epidemiological

characteristics typical of venereal diseases. Male plants with relatively many flowers have a greater incidence of disease than those plants with fewer flowers, perhaps because larger floral displays attract more pollinators and, thus, increase the likelihood of infection (Alexander and Antonovics, 1988; Alexander, 1989). If flower number has a genetic component, then there is a positive genetic correlation between potential fecundity and loss of fitness by disease: in effect, genes for low fecundity enhance resistance.

Berenbaum *et al.* (1986) found that, in addition to defensive chemicals, the flowering date of wild parsnips is correlated with damage by parsnip webworms. Those plants flowering early had less damage and many more seeds apparently because the number of herbivores increases as the season progresses. Flowering date is a heritable trait and there are phenotypic correlations among flowering date and the chemical components of resistance. There is not enough information to determine all the costs and benefits associated with flowering date. One possibility is that flowering early allows escape from herbivores in time but suffers greater risk of an early killing frost.

Biotic costs occur when a trait increases success against one race or species but reduces success against another. The idea that there are fitness trade-offs in multispecies interactions has been stressed repeatedly (Gould, 1983; Mitter and Futuyma, 1983; Marquis and Alexander, 1992), for example, when a parasite's fitness on two different hosts has a negative genetic correlation (Via, 1991; Fry, 1992). No theoretical studies have analysed the joint dynamics of population demography and genetics for these types of fitness trade-offs in quantitative traits.

The number of traits involved in an interaction may, in addition to costs, play an important role in maintaining genetic diversity. Each host trait may, for example, vary continuously but have a qualitative effect such that a certain threshold of resistance at any point of defence is sufficient to repel an attack. Multilocus qualitative resistance is known to maintain extensive polymorphism both in theory (Leonard and Czochor, 1980; Frank, 1993) and in the wild (Burdon, 1987).

The three types of fitness cost – metabolic, life history, and biotic – and the extension to multitrait interactions define a simple classification for the next phase of theoretical and empirical work. The model presented here provides a starting point for identifying the common and unique features among the dynamical properties of more realistic systems.

Acknowledgements

My research is supported by National Science Foundation grant BSR-9057331 and National Institutes of Health grants GM42403 and BRSG-S07-RR07008.

References

Note Added in Proof

Seger (1992) and Saloniemi (1993) have recently published coevolutionary models with quantitative characters.

Alexander, H.M. (1989) An experimental field study of anther-smut disease of *Silene alba* caused by *Ustilago violacea*: genotypic variation and disease resistance. *Evolution* **43**, 835–47.

Alexander, H.M. (1990) Dynamics of plant–pathogen interactions in natural plant communities. In *Pests, Pathogens and Plant Communities* (J.J. Burdon and S.R. Leather, eds), pp. 31–45. Blackwell Scientific, Oxford, UK.

Alexander, H.M. and Antonovics J. (1988) Disease spread and population dynamics of anther-smut infection of *Silene alba* caused by the fungus *Ustilago violacea*. *J. Ecol.* **76**, 91–104.

Berenbaum, M.R. and Zangerl, A.R. (1992) Quantification of chemical coevolution. In *Plant Resistance to*

Herbivores and Pathogens (R.S. Fritz and E.L. Simms, eds), pp. 69–87. University of Chicago Press, Chicago, USA.

Berenbaum, M.R., Zangerl, A.R. and Nitao, J.K. (1986) Constraints on chemical coevolution: wild parsnips and the parsnip webworm. *Evolution* **40**, 1215–28.

Burdon, J.J. (1987) *Diseases and Plant Population Biology*. Cambridge University Press, Cambridge, UK.

Christ, B.J., Person, C.O. and Pope, D.D. (1987) The genetic determination of variation in pathogenicity. In *Populations of Plant Pathogens* (M.S. Wolfe and C.E. Caten, eds), pp. 7–19. Blackwell Scientific, Oxford, UK.

Frank, S.A. (1990) Sex allocation theory for birds and mammals. *Ann. Rev. Ecol. System.* **21**, 13–55.

Frank, S.A. (1991a) Spatial variation in coevolutionary dynamics. *Evol. Ecol.* **5**, 193–217.

Frank, S.A. (1991b) Ecological and genetic models of host–pathogen coevolution. *Heredity* **67**, 73–83.

Frank, S.A. (1992) Models of plant–pathogen coevolution. *Trends Genet.* **8**, 213–19.

Frank, S.A. (1993) Coevolutionary genetics of plants and pathogens. *Evol. Ecol.* **7**, 45–75.

Frank, S.A. and Slatkin, M. (1990) The distribution of allelic effects under mutation and selection. *Genet. Res.* **55**, 111–17.

Fry, J.D. (1992) On the maintenance of genetic variation by disruptive selection among hosts in a phytophagous mite. *Evolution*, **46**, 279–83.

Gould, F. (1983) Genetics of plant–herbivore systems: interactions between applied and basic studies. In *Variable Plants and Herbivores in Natural and Managed Systems* (R.F. Denno and M.S. McClure, eds), pp. 599–653. Academic Press, New York, USA.

Guckenheimer, J. and Holmes, P. (1983) *Nonlinear Oscillations, Dynamical Systems, and Bifurcations of Vector Fields*. Springer-Verlag, New York, USA.

Hamilton, W.D. (1986) Instability and cycling of two competing hosts with two parasites. In *Evolutionary Processes and Theory* (S. Karlin and E. Nevo, eds), pp. 645–68. Academic Press, New York, USA.

Kennedy, G.G. and Barbour, J.D. (1992) Resistance variation in natural and managed systems. In *Plant Resistance to Herbivores and Pathogens* (R.S. Fritz and E.L. Simms, eds), pp. 13–41. University of Chicago Press, Chicago, USA.

Leonard, K.J. and Czochor, R.J. (1980) Theory of genetic interactions among populations of plants and their pathogens. *Ann. Rev. Phytopathol.* **18**, 237–58.

Marquis, R.J. and Alexander, H.M. (1992) Evolution of resistance and virulence in plant–herbivore and plant–pathogen interactions. *Trends Ecol. Evol.* **7**, 126–9.

May, R.M. (1974) *Stability and Complexity in Model Ecosystems*, 2nd edn. Princeton University Press, Princeton, NJ, USA.

Mitter, C. and Futuyma, D.J. (1983) An evolutionary–genetic view of host-plant utilization by insects. In *Variable Plants and Herbivores in Natural and Managed Systems* (R.F. Denno and M.S. McClure, eds), pp. 427–59. Academic Press, New York, USA.

Rausher, M.D. and Simms, E.L. (1989) The evolution of resistance to herbivory in *Ipomoea purpurea*. I. Attempts to detect selection. *Evolution* **43**, 563–72.

Saloniemi, I. (1993) A coevolutionary predator–prey model with quantitative characters. *Am. Nat.* **141**, 880–96.

Seger, J. (1992) Evolution of exploiter–victim relationships. In *Natural Enemies: the Population Biology of Predators, Parasites and Diseases* (M.J. Crawley, ed) pp. 3–25. Blackwell Scientific, Oxford, UK.

Simms, E.L. and Fritz, R.S. (1990) The ecology and evolution of host-plant resistance to insects. *Trends Ecol. Evol.* **5**, 356–60.

Simms, E.L. and Rausher, M.D. (1987) Costs and benefits of plant resistance to herbivory. *Am. Nat.* **130**, 570–81.

Simms, E.L. and Rausher, M.D. (1989) The evolution of resistance to herbivory in *Ipomoea purpurea*. II. Natural selection by insects and costs of resistance. *Evolution* **43**, 573–85.

Slatkin, M. (1987) Heritable variation and heterozygosity under a balance between mutation and stabilizing selection. *Genet. Res.* **50**, 53–62.

Via, S. (1991) The genetic structure of host plant adaptation in a spatial patchwork: demographic variability among reciprocally transplanted pea aphid clones. *Evolution* **45**, 827–52.

Wolfram, S. (1991) *Mathematica*, 2nd edn. Addison-Wesley, Redwood City, CA, USA.